a NASA facsimile reproduction

OF

N 65 88499

(ACCESSION NUMBER)

19

(PAGES)

CR-55411

(NASA CR OR TMX OR AD NUMBER)

(THRU)

None

(CODE)

(CATEGORY)

FACILITY FORM 602

REPRODUCED FROM MICROFORM

by the

Scientific and Technical Information Facility

N 112181
c 2.

MONTHLY PROGRESS REPORT NO. 4

Covering Period from November 1, 1963 to November 30, 1963

Contract NAS 3-2789

[redacted]

BRAYTON CYCLE SOLAR COLLECTOR
DESIGN STUDY PROGRAM
Item II. A.

[redacted]

THOMPSON RAMO WOOLDRIDGE INC.
New Product Research
Cleveland, Ohio

Project 512-08 4235-08

December 13, 1963
Date

0830
Department

[redacted]

TAPCO a division of Thompson Ramo Wooldridge Inc.

1.0 PROGRESS DURING THE REPORTING PERIOD

1.1 Summary of Overall Study Progress and Recommended Design

The major study and analysis tasks have been completed and the results establish that the design concept shown in figure 1.1-1 should be finalized in the detail d design and layout phase of the program.

The design concept consists of a continuous 1/4 inch thick reflector shell made-up of light weight aluminum honeycomb sandwich material. This reflector shell would be supported at the outer diameter by a continuous skirt and web type ring attached to the back of the shell and internally stiffened by honeycomb core material (see figure 1.3-2).

The honeycomb shell crossection is made-up of an .008 inch stretched formed aluminum reflective face in conjunction with 1/4 inch aluminum hexagonal cell core material and a .004 inch aluminum back face.

The approximate weight of this recommended design is as follows:

Shell	235 lbs.
Ring	190 lbs.
Total Structure	425 lbs.

This is approximately 0.60 lb/per square foot of intercepted area (706.7 sq. ft).

The structural analysis has shown that for the specified environmental loadings the superior structural efficiency makes aluminum honeycomb sandwich material a highly desirable structural concept for the Brayton Cycle concentrator. It has been indicated by specimen fabrication and inspections that with an .008 inch face material and proper fabrication process control a high optical quality honeycomb structure can be obtained. Thermoelastic analysis and specimen testing with imposed thermal gradients have shown that the thermal environment distortions are well within the optical quality requirements of the Brayton concentrator.

To determine performance optimization, surface error evaluations have resulted in a normal distribution surface error model. Computer solutions for this model

results in the optimum rim angle selection of 55° (see figure 1.2-3). Predicted performance of this concentrator is being computed. The combined concentrator-receiver performance shown in figure 1.2-4 is typical for a Brayton Cycle concentrator of the recommended design.

1.2 Performance Analysis

1.2.1 Concentrator Theoretical Analysis

The Aerospace Corporation developed computer analysis of solar reflectors which was discussed in last month's progress report has been utilized during this reporting period to perform the parametric calculations required for the Brayton collector study. It was decided to adopt this analytical tool in order to accelerate calculations and evaluations and because the accuracy and potential of this analysis is superior to the initial modified Silvern approach.

A copy of the program was obtained from Aerospace Corporation and the TRW computer facilities which are available at Space Technology Laboratories were utilized to compute the results.

The computer program considers imperfect concentrators with error distributions in two directions (radial and circumferential). Also considered are orientation errors and displacement [illegible] the focal plane. The computer prints out the flux concentration [illegible] the focal plane and the fraction of total incident energy collected within various aperture diameters.

A parametric study was established to investigate the following:

1. Surface accuracy
2. Concentrator diameter
3. Concentrator rim angle
4. Misorientation
5. Displacement of the receiver
6. Receiver characteristics

To minimize computer time the rim angle optimization computations were based upon the 9 minute radial standard deviation model as established from surface error evaluations. The 30 foot diameter concentrator was used in the calculations; however, the same order of magnitude surface deviations can be assumed for the 2 foot concentrator. The results are plotted showing a dimensionless scale so that other sizes can also be evaluated.

The following computer runs were performed:

Rim Angle	Std. Deviation	Misorientation
45°	9'	0
50°	9'	0
55°	9'	0
60°	9'	0
50°	9'	.25°
60°	9'	.25°

Results of varing rim angle for the oriented and maximum misorientation cases are shown in figures 1.2-1 and 1.2-2. It is seen that for the range of concentrator geometric efficiencies which are of interest (greater than 90%) the rim angles of 5 ° to 55° display a slightly more efficient characteristic. This is better demonstrated on the expanded scale shown in figure 1.2-3.

To investigate overall performance characteristics of the solar collection system, the combined concentrator-receiver efficiency is shown in figure 1.2-4. Since receiver geometry is not specified at this time, the receiver characteristics are based upon effective black body radiation levels. In this way, the effect of receiver temperature can be estimated. Calculations have been initiated for a cylindrical cavity configuration.

Predicted concentrator performance cases for the finalized 55° rim angle selection are being computed. With these results and a cavity geometry, the variation of combined efficiency with temperature and misorientation can be predicted.

1.2.2 Surface Error Evaluations

Data analysis of the surface error inspections of the five foot diameter stretch formed concentrator has been completed. Typical results are shown in figures

1.2-5, 6, and 7. The normal distribution characteristic is apparent and supports the original error model selected for the Brayton study.

The magnitudes of the measured deivations have been extrapolated to the larger diameter concentrators; and, in conjunction with other fabrication process considerations and estimated orbital environmental errors, the following surface error model was established:

Standard deviation (radial)	σ_r = 9' (68% of the surface)
Standard deviation (circum.)	σ_c = 4.5'
Maximum deviation	γ = 18' (95% of the surface)

This model is shown to be well within the present capabilities of the stretched formed concentrator technology. Smaller deviation cases will be considered in the computer optical analysis to determine performance limits.

To obtain a detailed investigation of the cell markoff characteristics normally associated with the recommended honeycomb sandwich structural design, an inspection arrangement and specimens have been fabricated. The arrangement consists of an insulated specimen holder, a heat source and a heat sink mounted on a Proficorder waviness inspection instrument. The honeycomb specimens, with thermocouples attached to the core and face, are subjected to various thermal gradients and levels, and any changes in shape are recorded by the waviness measurements.

Preliminary results indicate that optical face thickness in the range of .008 to .010 inches has negligible cell distortion characteristics. Proper fabrication processing is seen to be an important parameter in obtaining optically accurate honeycomb sandwich material.

1.3 Structural Analysis

1.3.1 Load Summary

Loads based on the Brayton Cycle Environmental Specification have been finalized. The load that will cause shell failure through buckling has been taken equal to 3 G plus 0.050 psi to allow for sound pressure and, or, the minimum thickness handling aspects of the problem. Stresses the ring and shell see result from

50 G acceleration plus 0.050 psi. This will cover shock and vibration (assuming the use of vibration isolators) as well as the 7 G axial acceleration; buckling of the shell is not assumed impending under this load.

1.3.2 Shell Construction

Several approaches to counteracting shell instability have been considered, including stabilization with either central column or many internal supports. A concentrator shell of honeycomb sandwich will be the lightest in weight as well as the most structurally reliable. The honeycomb crossection presented in Section 1.1 has been established as the recommended structural design. Analysis during this month's reporting period indicates that temperature levels and gradients as well as stresses for this crossection will be small. Objections to honeycomb in solar concentrators because of resulting fatigue or creep are therefore without foundation.

1.3.3 Thermal Stress Considerations

In last month's progress report it was concluded that the thin shell structure of the reflector will remain almost entirely distortion free due to a temperature gradient through the thickness. During this reporting period, other thermal gradients and discontinuities were investigated as well as the detailed consideration of the core to adhesive to face thermal environment.

1.3.3.1 Shell Thickness Temperature Gradient

The case considered is where the reflecting face temperature is greater than the back face temperature due to the temperature drop across the adhesive. The free thermal strain is resisted by internal stress in each face because of shell curvature effects. The stress is about 100 psi per °F difference in temperature, compression in the reflecting face and tension in the back face. The resulting moment maintains a distortion free surface.

The honeycomb core material strains almost freely in the plane of the panel or shell; shear stress requirements of the adhesive are, therefore, negligible.

Near the edge or rim of the concentrator, the support ring is required to provide the moment necessary to maintain a distortion free surface For the support rings considered and the 1/4 inch honeycomb section, the ring-shell junction will rotate about 0.3 minutes per °F. This edge distortion decays to zero within 8 or 10 inches of shell arc length from the edge.

1.3.3.2 Stresses at the Facing-Adhesive Bond

The facing-adhesive stresses are a consideration regardless of the fact that the restraint offered the adhesive by the honeycomb core is negligible. The adhesive will have a different coefficient of thermal expansion than the aluminum; in addition, there will be a small temperature difference between the two. An analysis of a ring of adhesive bounding a honeycomb cell face of 0.008 inch aluminum resulted in the following conclusions:

a. Bonding at room temperature results in only negligible tensile stress in the aluminum face if the section sees a temperature increase.

b. Assuming representative adhesive and aluminum characteristics, about 50 psi shear per 100 °F temperature change will exist in the adhesive. This stress is small, but the direction to go if improvement is required is as follows. Try to match coefficients of expansion, then select an adhesive with a low modulus of elasticity so that it can deform with with the metal without high stress build up.

c. The temperature gradient problem is similar to that of the two materials with the different coefficients that see a uniform change in temperature. Gradients of several degrees, are unimportant, therefore, compared to average temperature changes of 100 or 200°F.

1.3.3.3 Shell Radial Temperature Gradient

For the approximate radial temperature gradient as established from thermal analysis considerations (see figure 1.4-4), the distortion has been estimated by comparison of changes in focal length associated with the temperature extremes (refer to Progress Report No. 3 Section 1.4.1). Results show negligible effect on optics.

Should closer analysis show this radial gradient to be undesirable, it can be minimized by proper radiation control design as suggested in Section 1.4 of this report.

1.3.3.4 Support Ring - Shell Temperature Gradient

If the shell is at a temperature different than that of the ring, a redundant force and moment will be imposed on each at the ring-shell junction. Equating ring and shell displacements and rotations, respectively, allow the unknowns to be determined.

For a given ΔT, the shell edge rotates less with the ring on the back of the concentrator than on the front. With the ring on the back, about 0.3 minutes of edge rotation per °F can be expected from the redundant force and moment.

1.3.4 Shell Stresses During Launch

Axisymmetrical inertial or pressure loads will result in a meridian force (N_ϕ) that is maximum at the rim or edge of the concentrator. For the 30 foot dia collector, the relationship between the surface load and the edge force is, approximately,

$$N_\phi = 200\ P$$

The "high" stress load of 50 G plus 0.050 psi will result in

$$N_\phi = 12.0\ \#/\text{in.}$$

for the 1/4 inch honeycomb section considered. This edge force will result in a direct stress in the flanges of less than 3000 psi.

For the shallow shells considered, circumferential stresses will have the same sign as the meridian stresses but will be slightly smaller in magnitude.

To these membrane stresses must be added discontinuity stresses. Analysis that has just started indicates that they will be smaller than expected and may average only 10 to 20% of the membrane stress. This is probably due to the thinness of the shell section; it rotates slightly at the edge rather than resisting the angle change with resulting high stress.

1.3.5 Ring Considerations

Several configurations for the structural support ring have been considered.

For the eight point supported ring and a .2 #/in shell edge force loading, the crossection shown in figure 1.3-1 was shown to weigh less than the comparably designed circular crossection. The primary advantage of this crossection ring is the superior strength in the direction of the shell edge load. Other apparent advantages are:

1) The section is closed - this provides ample torsional rigidity.

2) The center of rotation of the section is closer to the edge of the shell than it would be for a circular section of comparable beam strength; the moment going into the ring is, therefore, less than it would be for the circular section.

3) The section is easy to fabricate. The outer flange is a circular cylinder. The web is a flat plate; the other is the shell itself. The honeycomb nose can be cut to the shape of the section and expanded in the circumferential direction.

4) Sufficient bond area is provided for the ring to sehll attachment. In addition, the transition from shell to ring is, or can be made, gradual. This should allow the full strength of the section to be developed.

5) The ring is on the back of the concentrator and will not intercept any solar energy. The ring does not extend beyond the rim of the concentrator; the full specified diameter can, therefore, be utilized to concentrate solar flux.

1.4 Thermal Analysis

The calculation of view factors for earth thermal and albedo radiation was completed for the concentrator and the support ring. Since an actual but not

an intercepted area was the basis of these calculations a geometric factor for the incident solar radiation was also determined. Using these factors as well as the data reported in progress report nos. 2 and 3, the total absorbed radiation was obtained. Figure nos. 1.4-1 to 1.4-3 show the absorbed radiation as a function of orbit time. The optical constants were the same as those used to calculate the transient temperatures in progress report no. 1, figures 4 and 5. As has been previously noted, the rotation of the power system results in a time average view factor for any radiation source which is not coaxial with the concentrator. No circumferential gradient in the absorbed energy will therefore occur. However, a radial gradient is experienced as shown by the different magnitudes shown in figures 1.4-1 to 1.4-3. To obtain an approximate temperature level as well as the resultant radial gradient, steady state temperatures of a single shell were calculated at the end of the sun time. The results are plotted as curve 1 of figures 1.4-4 and show a 24°F temperature gradient between the center and rim of the concentrator.

To obtain the temperature level and gradients of a honeycomb structure, vacuum test data obtained during the Sunflower program was used. The test results for a .375 hex by .5 thick structure have been reproduced on figure 1.4-5. Holding everything else constant, it was determined that the ΔT through the honeycomb is approximately proportional to the hex size. Making this correction, the proposed .25 hex size would produce a ΔT as shown by the second curve. The change in core thickness from .5 to .25 in. and the core material thickness from .001 to .0002 was not considered. The first would have only a minor effect on the total ΔT whereas the second could be appreciable. However no test results are available and no basis for a reasonable estimate exists. In any case the net effect would be to decrease the thermal gradient from that shown in figure 1.4-4.

Steady state temperatures of the honeycomb structure at the end of the sun time were calculated for two cases. The first case did not consider any side conduction whereas the second did. Both results are plotted on figure 1.4-4. No appreciable change is evident. Since the support ring will be an integral part of the structure, its temperature is also shown on this graph.

Thermal gradients in any structure will produce deflection or stresses or a combination of both. Deflections can only be tolerated as long as the geometric accuracy is not impaired. Thermal stress levels are of little consequence for the expected gradients. To reduce or even eliminate deflections the thermal gradients must be decreased, prevented or used to advantage.

Two ways of reducing the ΔT through the honeycomb would be the reduction in the adhesive bond resistance and the increase of the emissivity of the front face. Both show promise but should be evaluated experimentally. High conductivity adhesive have not been recommended for the Brayton concentrator honeycomb sandwich design because, as has been shown previously, the thermal distortion of a solid shell caused by a temperature differential through the thickness is localized at the OD and small in magnitude and therefore well within the optical quality requirements of the Brayton concentrator.

Radial temperature gradient can be eliminated quite easily by varying the total emissivity of the back side with radial position. This could be accomplished by covering portions of the area with multi-layer radiation barriers. Reducing the emissive surface would result in a higher overall temperature level. Covering about 5% of the area at the mid radius and increasing it to about 20% at the rim would result in constant face temperatures as shown in figure 1.4-6. Added weight would be about 5 lbs.

1.5 Micrometeoroid Erosion Investigation

The following reflector surface specimens have been prepared for simulated micrometeoroid erosion testing at NASA Lewis:

a. Aluminum substrate/Pure aluminum coating
b. Aluminum/Epoxy coat/Aluminum (600 Å)
c. Aluminum/Epoxy coat/Aluminum (2300 Å)
d. Aluminum/Epoxy/Aluminum (600 Å)/SiO (2300 Å)
e. Aluminum/Epoxy/SiO (3000 Å)/Aluminum (600 Å)/SiO (2300 Å)
f. Aluminum/Epoxy/SiO (3000 Å)/Aluminum (600 Å)/SiO (2 μ)

Reflectivity measurements of the specimens are being made by the Thermal Radiation Laboratory at Space Technology Laboratories, Inc. Near normal direction, total reflectance measurements are obtained with a modified Beckman DK-2A integrating sphere reflectometer; while the "diffuse" component of the reflectance is measured in a Gier-Dunkle integrating sphere at selected wave lengths within the solar spectrum.

"Micrometeoroid Considerations in Solar Collector Design", TRW Report TM-3841-68 has been prepared to correlate the available space environment parameters with a peretration-cratering characteristic as related to the specific Brayton Cycle concentrator design, and for comparison with NASA Lewis shock tube experimental results. General conclusions are:

1. Unknowns of the exact space environment and resulting penetration-cratering phenomenon produce a wide range of predictable degradation.

2. Depending upon the actual penetration-cratering characteristic, the NASA Lewis shock tube experiment produce 6.5 times as much area degradation as the actual high velocity micrometeoroid particles - although volume degradation remains the same.

Specific suggestions are made for more exploratory and conclusive utilization of the shock tube experiments.

2.0 PROBLEM AREAS AND CORRECTIVE ACTION

Although the major study tasks have been completed, the finalization and predicted performance tasks have extended into December.

Receiver geometry finalization is necessary to predict combined collection efficiency. The cylindrical cavity configuration will be investigated for study purposes.

3.0 WORK TO BE PERFORMED DURING THE NEXT MONTH

As shown in the attached task schedule, optimization and final predicted performance

tasks will be completed. The recommended Brayton Cycle concentrator design concept will be presented to NASA Lewis for discussion and approval. Preliminary layouts of the design will begin.

Micrometeoroid erosion specimens will be delivered to NASA Lewis for shock tube experiments.

TASK SCHEDULE [redacted]

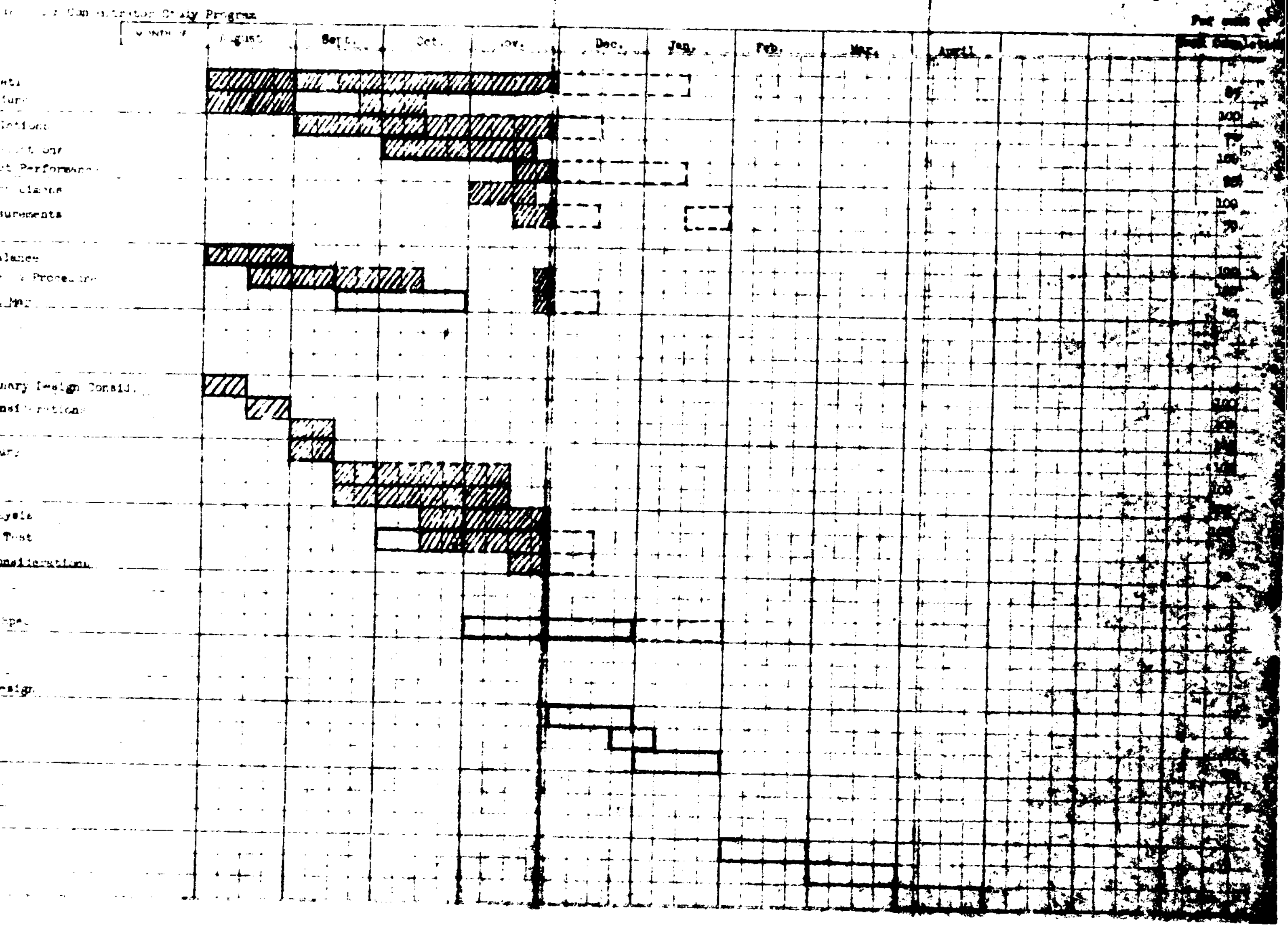

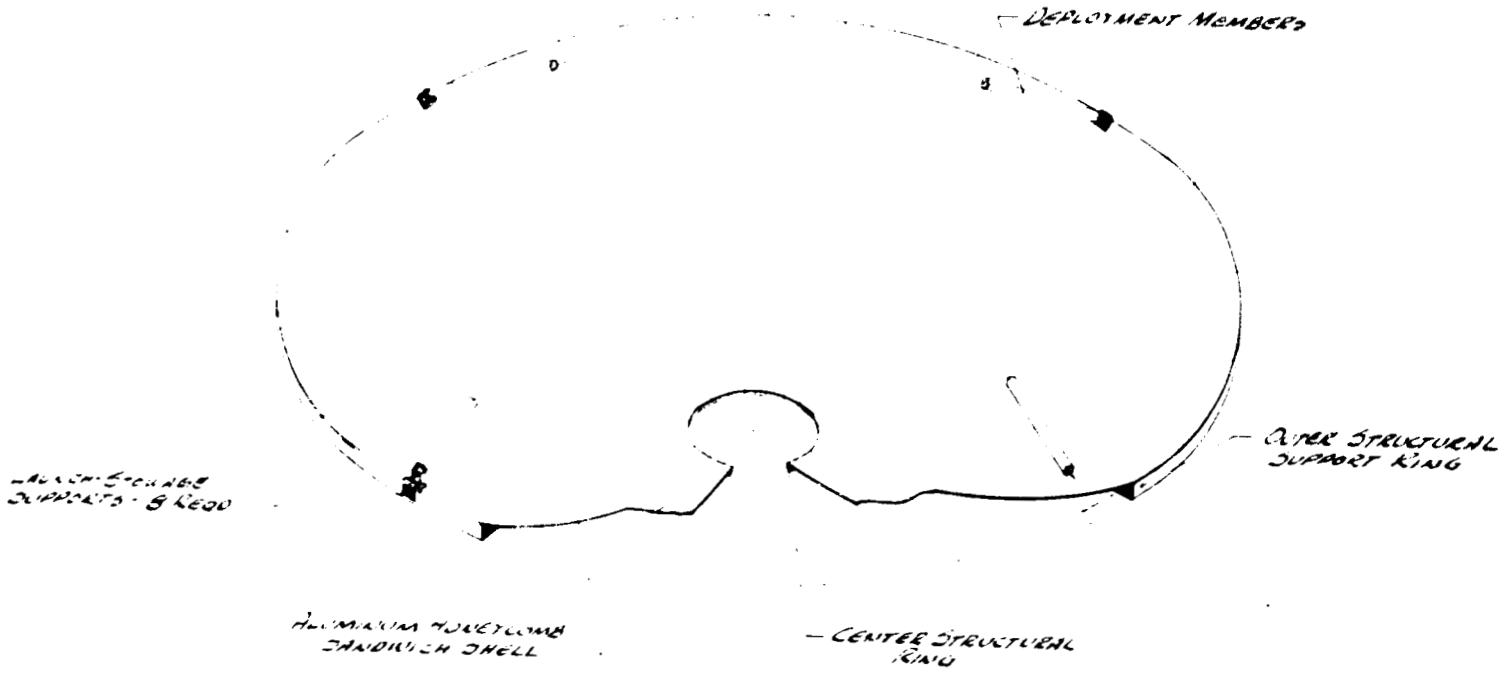

BRAYTON CYCLE CONCENTRATOR - DESIGN CONCEPT

FIG. 1.1-1
DUP 12-13-63

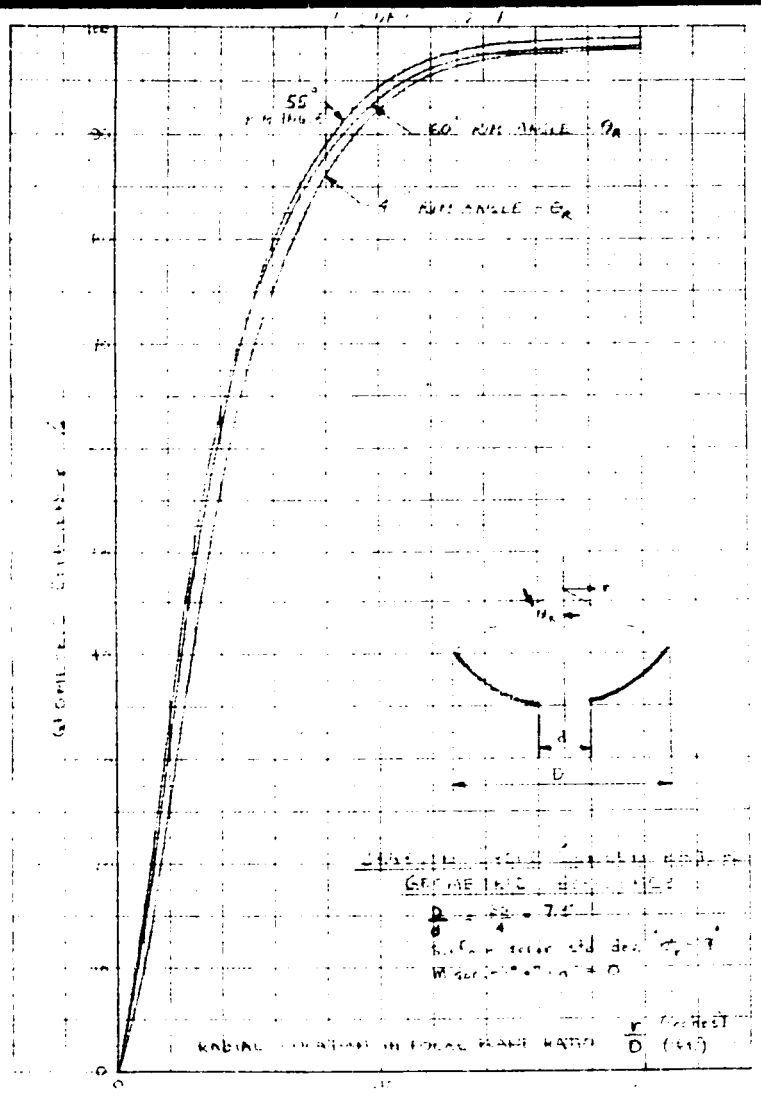
55°
60° RIM ANGLE θ_R
RIM ANGLE = θ_R
d
D

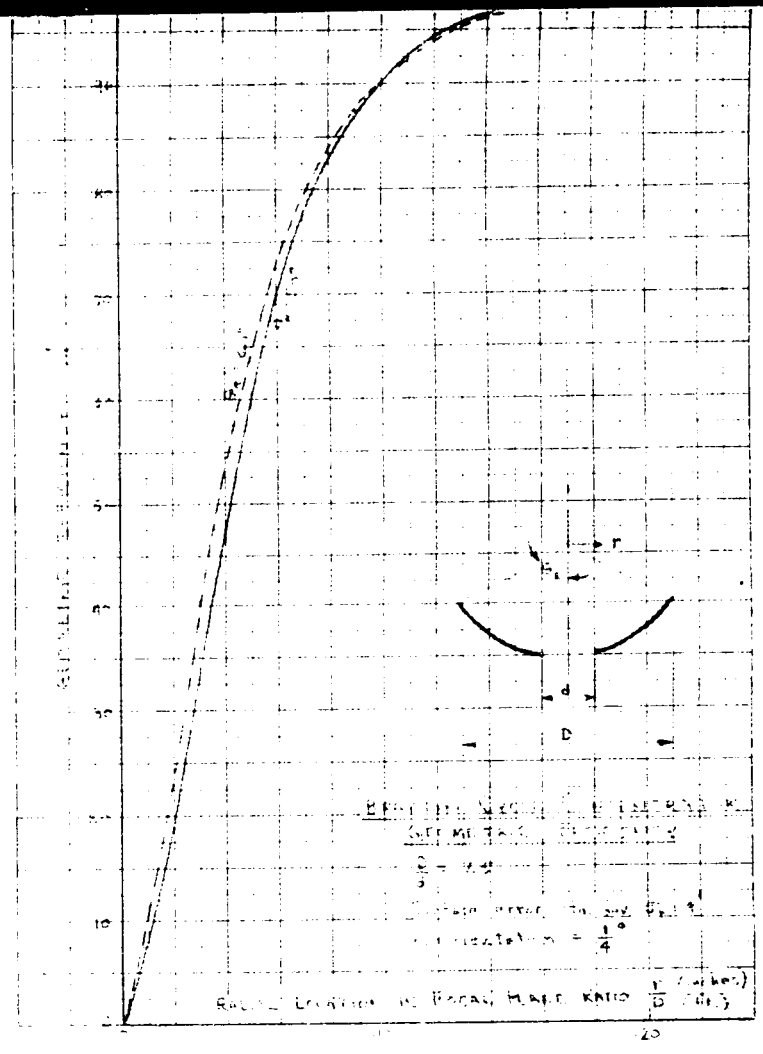
d
D

FIGURE 1.2-5

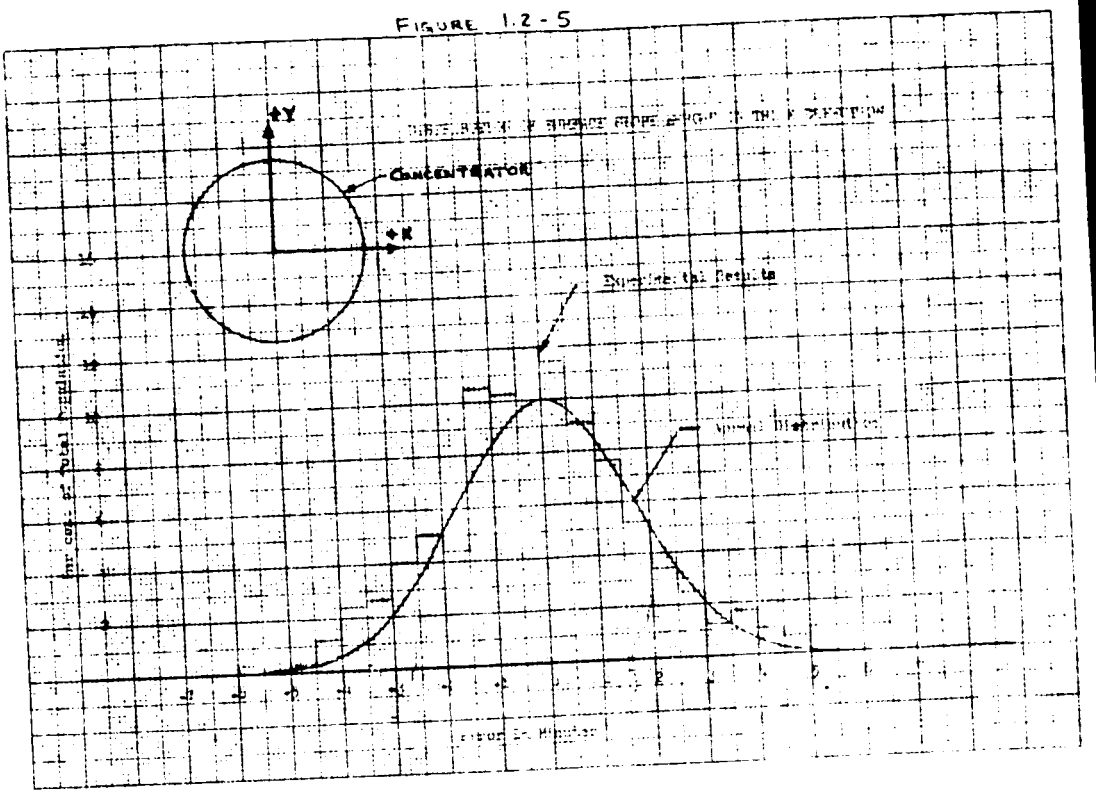

K+E

FIGURE 1.2-6

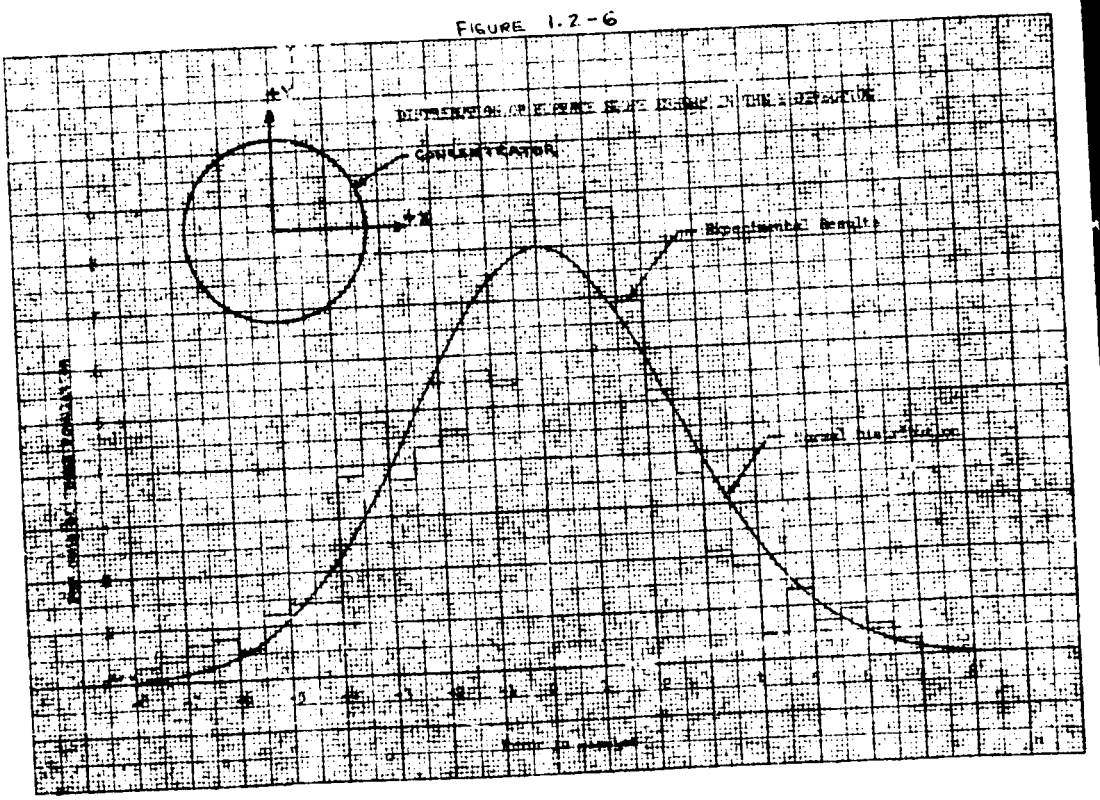

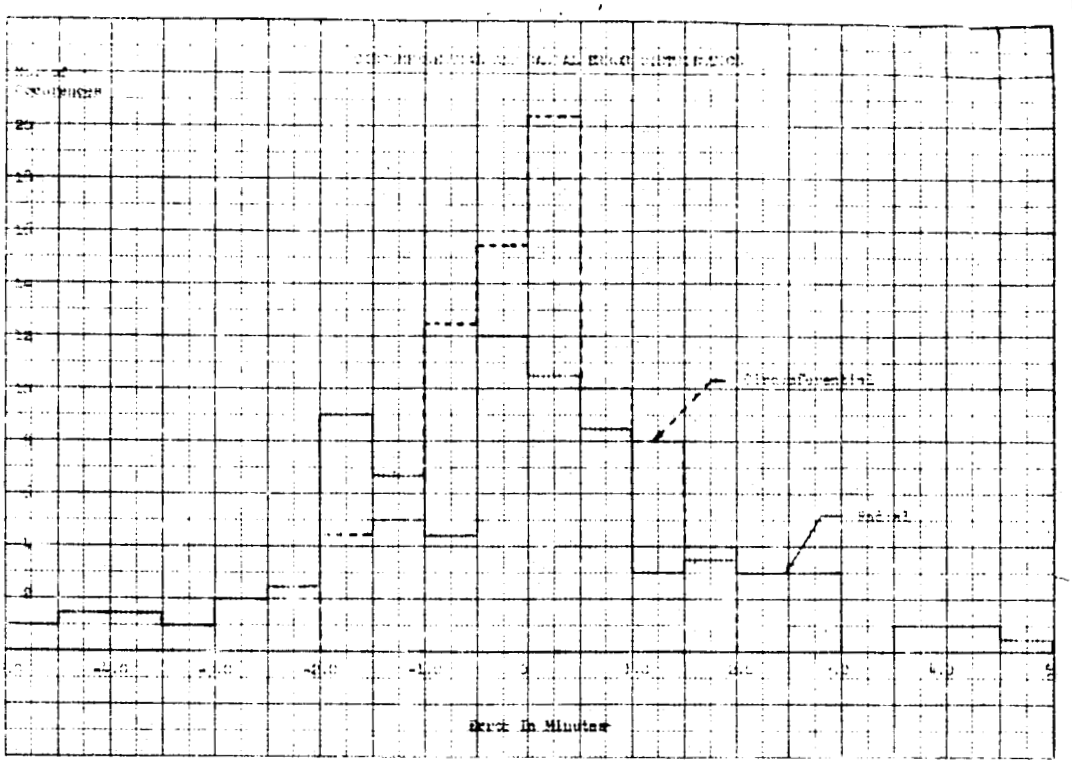
Error In Minutes

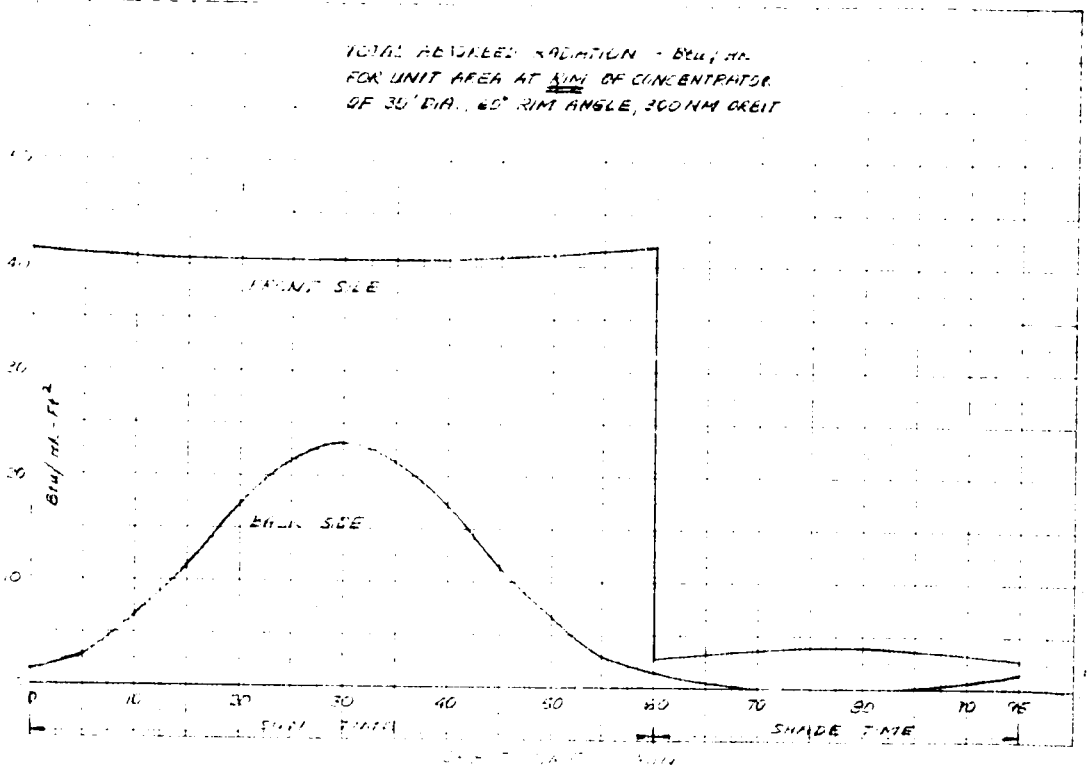
TOTAL REVERSED RADIATION - BTU/HR.
FOR UNIT AREA AT RIM OF CONCENTRATOR
OF 30' DIA., 60° RIM ANGLE, 200 NM ORBIT
FRONT SIDE
BACK SIDE
BTU/HR.-FT²
0
10
20
30
40
50
60
70
80
90
100
SHADE TIME

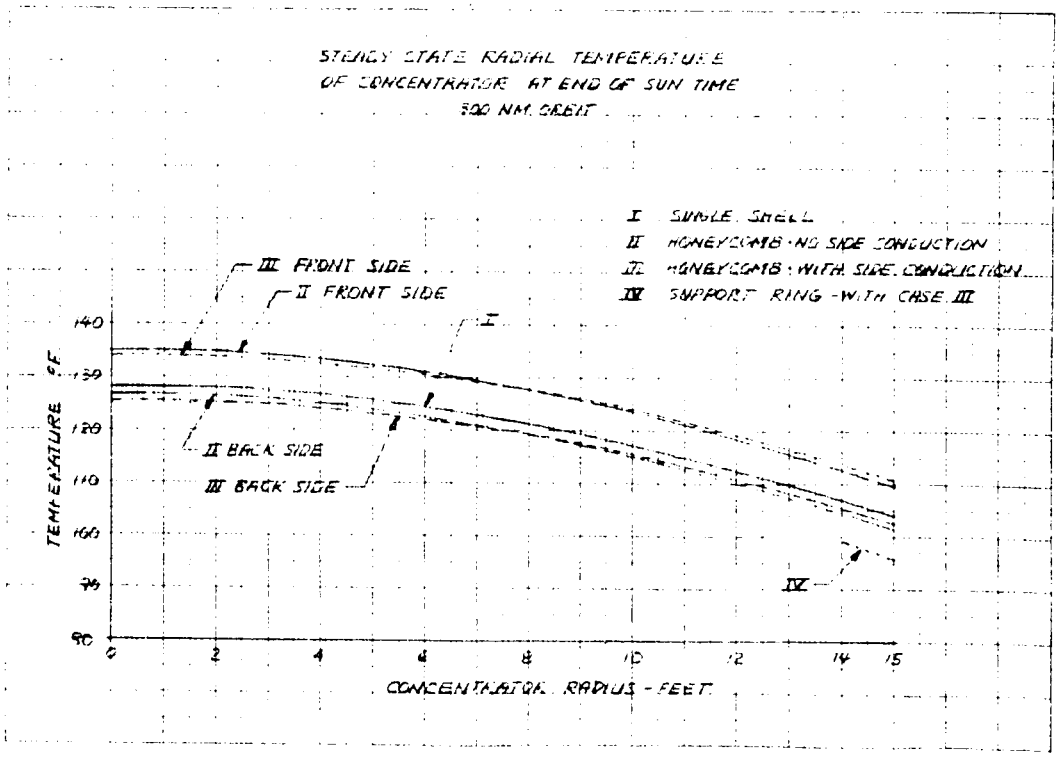
STEADY STATE RADIAL TEMPERATURE
OF CONCENTRATOR AT END OF SUN TIME
200 NM ORBIT
I SINGLE SHELL
II HONEYCOMB - NO SIDE CONDUCTION
III HONEYCOMB - WITH SIDE CONDUCTION
IV SUPPORT RING - WITH CASE III
III FRONT SIDE
II FRONT SIDE
I
II BACK SIDE
III BACK SIDE
IV
TEMPERATURE °F
140
130
120
110
100
90
0
2
4
6
8
10
12
14
15
CONCENTRATOR RADIUS - FEET

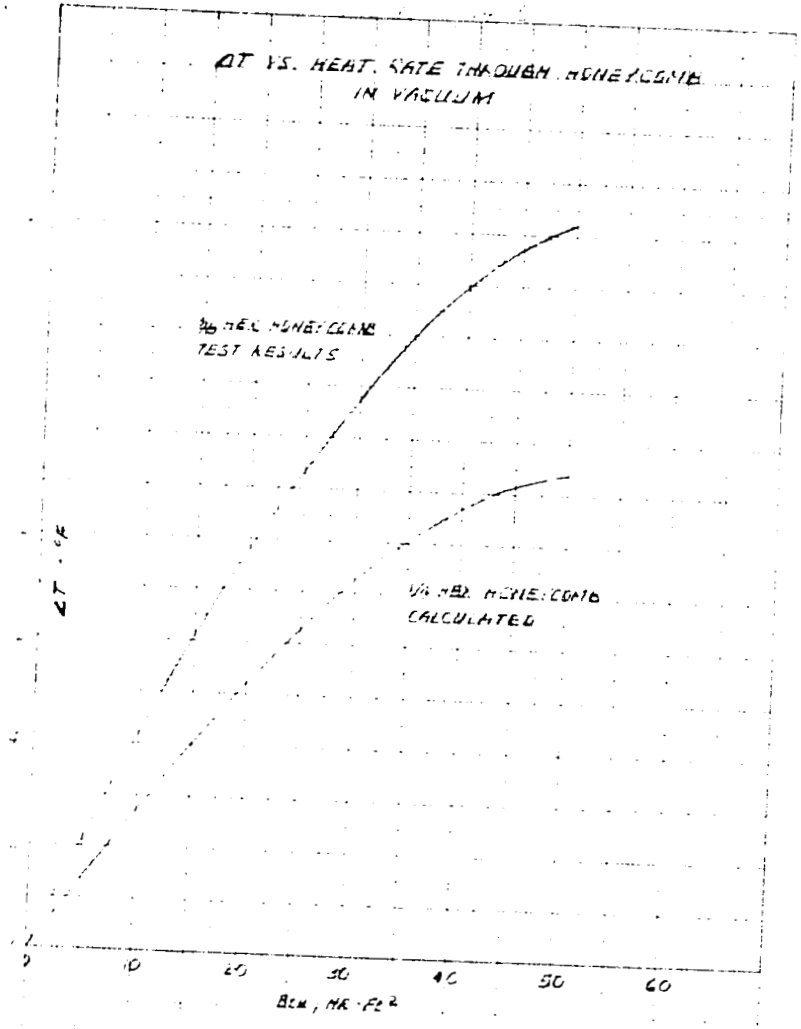
ΔT VS. HEAT RATE THROUGH HONEYCOMB
IN VACUUM
3/8 HEX HONEYCOMB
TEST RESULTS
1/4 HEX HONEYCOMB
CALCULATED
ΔT - °F
0
10
20
30
40
50
60
BTU, HR-FT²

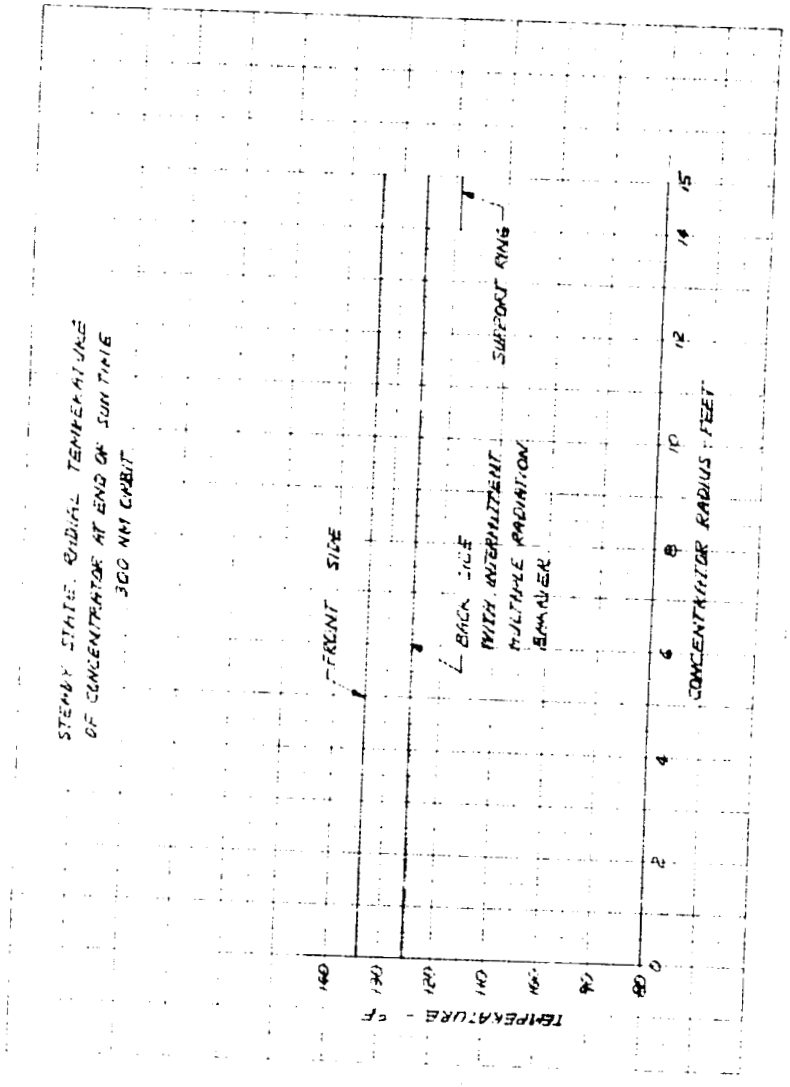
STEADY STATE RADIAL TEMPERATURE
OF CONCENTRATOR AT END OF SUN TIME
300 NM ORBIT
FRONT SIDE
BACK SIDE
WITH INTERMITTENT
MULTIPLE RADIATION
BANDER
SUPPORT RING
TEMPERATURE - °F
140
130
120
110
100
90
80
0
2
4
6
8
10
12
14
15
CONCENTRATOR RADIUS - FEET